

# HEAT AND MASS TRANSFER WITH CHEMICAL REACTION EFFECTS ON MHD FREE CONVECTION FLOW THROUGH A MOVING PERMEABLE VERTICAL SURFACE EMBEDDED IN A POROUS MEDIUM

UMA SHANKER, HEMANT POONIA & S. S. DHAYAL

Assistant Professor, Department of Mathematics and Statistics,  
Chaudhary Charan Singh Haryana Agricultural University, Hisar, Haryana, India

## ABSTRACT

*In this paper, an analysis is performed to study the momentum, heat and mass transfer characteristics of MHD natural convection flow over a moving permeable surface. The surface is maintained at linear temperature and concentration variations. The non-linear coupled boundary layer equations were transformed and the resulting ordinary differential equations were solved by perturbation technique. The solution is found to be dependent on several governing parameters, including the magnetic field strength parameter, Prandtl number, Schmidt number, buoyancy ratio and suction/blowing parameter, a parametric study of all the governing parameters is carried out and representative results are illustrated to reveal a typical tendency of the solutions. Numerical results for the dimensionless velocity profiles, the temperature profiles, the concentration profiles, the local friction coefficient and the local Nusselt number are presented in various combinations of parameters.*

**KEYWORDS:** Heat and Mass Transfer, Chemical Reaction, MHD, Porous Medium & Free Convection

**Received:** Apr 20, 2018; **Accepted:** May 14, 2018; **Published:** June 08, 2018; **Paper Id.:** IJMCARJUN20182

## 1. INTRODUCTION

Hydromagnetic incompressible viscous flow has many important engineering applications such as magneto fluid hydrodynamic power generator and the cooling of reactors. Tsou et al. [III] Considered the effect of heat transfer on a continuous moving surface with a constant velocity and experimentally confirmed the numerical results of Sakiadis. Chen and Strobel [IV] considered the effect of a buoyancy induced pressure gradient in a laminar boundary layer of a stretched sheet with constant velocity and temperature. Chakrabarti and Gupta [V] studied the MHD flow of Newtonian fluids initially at rest, over a stretching sheet at a different uniform temperature. Vajravelu and Hadjinicolaou [VI] made an analysis of flows and heat transfer characteristics in an electrically conducting fluid near an isothermal sheet. Cheng and Huang [VII] considered the problem of unsteady flows and heat transfer in the laminar boundary layer on a linearly accelerating surface with suction or blowing in the absence and presence of a heat source or sink. Xu and Liao [VIII] investigated the un-steady MHD flows of a non-Newtonian fluid over a non-impulsively stretching flat sheet and presented an accurate series solution. Some works are available on the subject of magneto-hydrodynamic (MHD) convection in porous medium was studied by Abdelkhalek [IX–XI]. The problem of magneto-hydrodynamic natural convection about a vertical impermeable flat plate is presented by Wilks and Hunt [XII]. Watanabe and Pop [XIII] studied the case of a wedge. Kafoussias [XIV] investigated the MHD free convective flow through a porous medium over an isothermal cone

surface. Bakier et al. [XV] Presented non-similar solutions for free convection from a vertical permeable plate in porous media. Similarity solutions of natural convection boundary layers adjacent to vertical and horizontal surfaces in porous media with internal heat generation were studied by Pop [XVI]. Grubka and Bobba [XVII] investigated heat transfer characteristics of a continuous, stretching surface with variable wall temperature Ali [XVIII] numerically presented the heat transfer characteristics of a power law continuous stretched surface without and with suction injection. Takhar et al [XIX]. Studied a MHD symmetric flow past a semi infinite moving plate and numerically obtained the solutions Yih [XX] studied a free convection effect on MHD coupled heat and mass transfer of a moving permeable vertical surface.

The main objective of this analysis investigates the effect of heat and mass transfer in a hydro-magnetic flow of a moving permeable vertical surface. In the formulation of the problem, it can be demonstrated that the system of momentum, heat and mass conservation equations can be reduced to some parameter problem by introducing suitable transformation variable. The resulting transformed governing equations are then solved using a perturbation technique [I]. Typical results for the velocity, temperature and concentration profiles are presented for various governing parameters. Also the local skin-friction coefficient as well as the heat and mass transfer results is illustrated for representative values of the major parameters.

## 2. MATHEMATICAL FORMULATION

Let us consider the two-dimensional free convection effect on the steady incompressible laminar MHD heat and mass transfer characteristics of a linear moving permeable vertical surface when the velocity of the fluid far away from the plate is equal to zero. The variations of surface temperature and concentration are linear. All the fluid properties are assumed to be constant except for the density variations in the buoyancy force term of linear momentum. The magnetic Reynolds number is assumed to be small so that the induced magnetic field is neglected. No electric field is assumed to exist and both viscous and magnetic dissipations are neglected. The Hall effect, the viscous dissipation, and the joule heating terms are also neglected. Under these assumptions, along with Boussinesq approximations, the boundary layer equations for this problem can be written as:

$$\frac{\partial u}{\partial X} + \frac{\partial v}{\partial Y} = 0 \quad (2.1)$$

$$u \frac{\partial u}{\partial X} + v \frac{\partial u}{\partial Y} = \nu \frac{\partial^2 u}{\partial Y^2} + g\beta(T - T_\infty) + g\beta_c(C - C_\infty) - \frac{\sigma B_0^2 u}{\rho} - \frac{uv}{\alpha} \quad (2.2)$$

$$u \frac{\partial T}{\partial X} + v \frac{\partial T}{\partial Y} = a_0 \frac{\partial^2 T}{\partial Y^2} \quad (2.3)$$

$$u \frac{\partial C'}{\partial X} + v \frac{\partial C'}{\partial Y} = D \frac{\partial^2 C'}{\partial Y^2} - K_1(C' - C_\infty) \quad (2.4)$$

The relative boundary condition can be written as

$$\left. \begin{aligned} y = 0, v = -V_w, u = BX, T = T_\infty + aX, C' = C_\infty + bX \\ y \rightarrow \infty, u = 0, T = T_\infty, C' = C_\infty \end{aligned} \right\} \quad (2.5)$$

Where  $V_w$  the uniform surface is mass flux and  $B, a$  and  $b$  are prescribed constants.

We introduce now the following non-dimensional variables

$$\begin{aligned} u &= \frac{\partial \psi}{\partial Y}, u = -\frac{\partial \psi}{\partial X}, \eta = \sqrt{\frac{B}{v}} Y, F(\eta) = \frac{\psi}{X \sqrt{Bv}}, \theta(\eta) = \frac{T - T_\infty}{T_w(X) - T_\infty}, \\ \theta(\eta) &= \frac{C' - C'_\infty}{C'_\infty(X) - C'_\infty}, \psi = XF(\eta) \sqrt{Bv}, u = BXF', v = -F(\eta) \sqrt{Bv}, \\ \alpha &= \frac{B\alpha'}{v}, K = \frac{K_1}{B}, S_c = \frac{v}{D}, M = \frac{\sigma B_0^2}{B\rho}, N = \frac{\beta_c b}{\beta a}, P_r = \frac{v}{a_0} \end{aligned} \quad (2.6)$$

With a new set of independent and dependent variable defined by equation (2.6), Equation (2.1) is identically satisfied, and the partial differential equations (2.2) to (2.4) transform into ordinary differential equations (2.7) to (2.9).

$$F''' + FF'' - \left( M + \frac{1}{\alpha} + F' \right) F' = -G_r R_e^{-2} (\theta + NC) \quad (2.7)$$

$$\theta'' + P_r (F\theta' - F'\theta) = 0 \quad (2.8)$$

$$C'' + S_c (FC' - F'C - KC) = 0 \quad (2.9)$$

Where primes denote differentiation with respect to  $\eta$ . The appropriate flat plate, free convection boundary conditions also transform into the form,

$$\left. \begin{aligned} \eta = 0, F &= F_w, F' = 1, \theta = 1, C = 1 \\ \eta \rightarrow \infty, F' &= 0, \theta = 0, C = 0 \end{aligned} \right\} \quad (2.10)$$

The velocity components are

$$u = BXF', v = -F\sqrt{B\xi}$$

Where  $M = \sigma B_0^2 B^{-1} q^{-1}$  is magnetic parameter,  $G_r R_e^{-2} = g \beta a B^{-2}$  is the buoyancy parameter, when  $G_r R_e^{-2} = 0$  the governing equation is reduces to the forced convection limit. However, as  $G_r R_e^{-2} \rightarrow \infty$  free convection is dominated. The buoyancy ratio  $N$  measures the relation importance of mass and thermal diffusion in the buoyancy driven flow. It is apparent that  $N$  is zero for thermal driven flow, infinite for mass driven flow, positive for thermally assisting flow, negative for thermally opposing flow,  $Pr$  is the Prandtl number and  $Sc$  is the Schmidt number,  $F_w = V_w / \sqrt{Bv}$  is the suction / blowing parameter. In the case of suction  $V_w > 0$  and  $F_w > 0$ . In the case of blowing  $V_w < 0$  and hence  $F_w < 0$ .

### 3. SOLUTION OF THE PROBLEM

The resulting differential equation contains arbitrary parameters, the Prandtl number, the magnetic field strength and buoyant force, the ratio of the Hartmann number is a measure of the relative influence of the magnetic and buoyant forces on the temperature and flow field. Solution of the resulting semi-infinite domain, non-linear equations is

accomplished with a three part series method [II]. The employed power series equation (3.1) contains a term A that satisfies the boundary condition and the differential equation at infinity, a second term that satisfied the boundary condition at zero and is the solution of initial homogeneous differential equations and additional terms that are utilized to obtain increased numerical accuracy. This accuracy is limited by the number of terms that will not initiate divergence of the numerical results.

$$\left. \begin{aligned} F &= A + \varepsilon F_1 + \varepsilon^2 F_2 + \varepsilon^3 F_3 + \dots \\ \theta &= \varepsilon \theta_1 + \varepsilon^2 \theta_2 + \varepsilon^3 \theta_3 + \dots \\ C &= \varepsilon C_1 + \varepsilon^2 C_2 + \varepsilon^3 C_3 + \dots \end{aligned} \right\} \quad (3.1)$$

Subject to the boundary conditions

$$\left. \begin{aligned} \eta = 0, F_1(0) = F_w, F_2(0) = F_3(0) = 0, F_1'(0) = 1, F_2'(0) = F_3'(0) = 0 \\ \theta_1(0) = 1, \theta_2(0) = \theta_3(0) = 0, C_1(0) = 1, C_2(0) = C_3(0) = 0 \\ \eta \rightarrow \infty, F_n'(\infty) = 0, \theta_n(\infty) = 0, C_n(\infty) = 0, \quad n = 1, 2, 3 \end{aligned} \right\} \quad (3.2)$$

Boundary conditions, equation (3.2), contain undetermined parameter  $\varepsilon$  which aides in the collection of terms for each set of the resulting linear differential equations. In some problems, it will have physical meaning which results in a power series in that parameter. However, the present case  $\varepsilon$  equals unity. Substitutions of the series representation into the differential equations and collection of terms by like powers of  $\varepsilon$  result in a family of linear differential equations, and the first three sets are

$$F_1'' + AF_1'' - \left( M + \frac{1}{\alpha} \right) F_1' = -G_r R_e^{-2} (\theta_1 + NC_1) \quad (3.3)$$

$$\theta_1'' + AP_r \theta_1' = 0 \quad (3.4)$$

$$C_1'' + AS_c C_1' - KC_1 = 0 \quad (3.5)$$

$$F_2'' + AF_2'' - \left( M + \frac{1}{\alpha} \right) F_2' = F_1' - F_1 F_1'' - G_r R_e^{-2} (\theta_2 + NC_2) \quad (3.6)$$

$$\theta_2'' + AP_r \theta_2' = P_r (F_1' \theta_1 - F_1 \theta_1') \quad (3.7)$$

$$C_2'' + AS_c C_2' - KC_2 = S_c (F_1' C_1 - F_1 C_1') \quad (3.8)$$

$$F_3'' + AF_3'' - \left( M + \frac{1}{\alpha} \right) F_3' = 2F_1' F_2' - F_2 F_1'' - F_1 F_2'' - G_r R_e^{-2} (\theta_3 + NC_3) \quad (3.9)$$

$$\theta_3'' + AP_r \theta_3' = P_r (F_1' \theta_2 + F_2' \theta_1 - F_1 \theta_2' - F_2 \theta_1') \quad (3.10)$$

$$C_3'' + AS_c C_3' - KC_3 = S_c (F_1' C_2 + F_2' C_1 - F_1 C_2' - F_2 C_1') \quad (3.11)$$

On solving equations (3.3) to (3.11) by using boundary conditions (3.2), we get the following solutions

$$\theta_1 = e^{-AP_r\eta} \quad (3.12)$$

$$C_1 = e^{-a_2\eta} \quad (3.13)$$

$$F_1 = a_5 + a_4e^{-a_3\eta} + a_6e^{-AP_r\eta} + a_7e^{-a_2\eta} \quad (3.14)$$

$$\theta_2 = a_{11}e^{-AP_r\eta} + a_8e^{-(a_3+AP_r)\eta} + a_9e^{-(a_2+AP_r)\eta} + a_{10}\eta e^{-AP_r\eta} \quad (3.15)$$

$$C_2 = a_{15}e^{-a_2\eta} + a_{12}e^{-(a_2+a_3)\eta} + a_{13}e^{-(a_2+AP_r)\eta} + a_{14}\eta e^{-a_2\eta} \quad (3.16)$$

$$F_2 = a_{36}e^{-a_3\eta} + a_{37} + a_{24}e^{-(a_3+AP_r)\eta} + a_{25}e^{-(a_2+AP_r)\eta} + a_{26}e^{-(a_2+a_3)\eta} + a_{27}\eta e^{-a_3\eta} \\ + a_{34}e^{-a_2\eta} + a_{29}\eta e^{-a_2\eta} + a_{35}e^{-AP_r\eta} + a_{32}\eta e^{-AP_r\eta} \quad (3.17)$$

$$\theta_3 = a_{64}e^{-AP_r\eta} + a_{51}e^{-(a_3+AP_r)\eta} + a_{52}\eta e^{-(a_3+AP_r)\eta} + a_{53}e^{-(a_2+AP_r)\eta} + a_{54}\eta e^{-(a_2+AP_r)\eta} \\ + a_{55}e^{-(a_2+a_3+AP_r)\eta} + a_{56}e^{-(2a_3+AP_r)\eta} + a_{57}e^{-(a_3+2AP_r)\eta} + a_{58}e^{-(2a_2+AP_r)\eta} + a_{59}e^{-(a_2+2AP_r)\eta} \\ + a_{60}e^{-2AP_r\eta} + a_{61}\eta e^{-2AP_r\eta} + a_{62}\eta e^{-AP_r\eta} + a_{63}\eta^2 e^{-AP_r\eta} \quad (3.18)$$

$$C_3 = a_{89}e^{-a_2\eta} + a_{77}e^{-(a_2+a_3)\eta} + a_{78}\eta e^{-(a_2+a_3)\eta} + a_{79}e^{-(a_2+a_3+AP_r)\eta} + a_{80}e^{-(a_2+2a_3)\eta} \\ + a_{81}e^{-(a_2+AP_r)\eta} + a_{82}\eta e^{-(a_2+AP_r)\eta} + a_{83}e^{-(a_2+2AP_r)\eta} + a_{84}e^{-(2a_2+a_3)\eta} + a_{85}e^{-(2a_2+AP_r)\eta} \\ + a_{86}e^{-2a_2\eta} + a_{87}\eta e^{-a_2\eta} + a_{88}\eta^2 e^{-a_2\eta} \quad (3.19)$$

$$F_3 = a_{142}e^{-a_3\eta} + a_{143} + a_{116}e^{-(a_3+AP_r)\eta} + a_{117}\eta e^{-(a_3+AP_r)\eta} + a_{118}e^{-(a_2+AP_r)\eta} + a_{119}\eta e^{-(a_2+AP_r)\eta} \\ + a_{120}e^{-(a_2+a_3+AP_r)\eta} + a_{121}e^{-(a_2+a_3)\eta} + a_{122}\eta e^{-(a_2+a_3)\eta} + a_{123}e^{-2a_3\eta} + a_{124}\eta e^{-2a_3\eta} + a_{125}e^{-2a_2\eta} \\ + a_{126}e^{-(2a_3+AP_r)\eta} + a_{127}e^{-(a_3+2AP_r)\eta} + a_{128}e^{-(2a_2+AP_r)\eta} + a_{129}e^{-(a_2+2AP_r)\eta} + a_{130}e^{-(a_2+2a_3)\eta} \\ + a_{131}e^{-2AP_r\eta} + a_{132}\eta e^{-2AP_r\eta} + a_{133}e^{-(2a_2+a_3)\eta} + a_{134}e^{-AP_r\eta} + a_{135}\eta e^{-AP_r\eta} + a_{136}\eta^2 e^{-AP_r\eta} \\ + a_{137}e^{-a_2\eta} + a_{138}\eta e^{-a_2\eta} + a_{139}\eta^2 e^{-a_2\eta} + a_{140}\eta e^{-a_3\eta} + a_{141}\eta^2 e^{-a_3\eta} \quad (3.20)$$

$$\theta_1' = -AP_re^{-AP_r\eta} \quad (3.21)$$

$$C_1' = -a_2e^{-a_2\eta} \quad (3.22)$$

$$F_1' = -a_3a_4e^{-a_3\eta} - AP_ra_6e^{-AP_r\eta} - a_2a_7e^{-a_2\eta} \quad (3.23)$$

$$\theta_2' = -AP_ra_{11}e^{-AP_r\eta} - (a_3 + AP_r)a_8e^{-(a_3+AP_r)\eta} - (a_2 + AP_r)a_9e^{-(a_2+AP_r)\eta} \\ + a_{10}e^{-AP_r\eta} - AP_ra_{10}\eta e^{-AP_r\eta} \quad (3.24)$$

$$C_2' = -a_2a_{15}e^{-a_2\eta} - (a_2 + a_3)a_{12}e^{-(a_2+a_3)\eta} - (a_2 + AP_r)a_{13}e^{-(a_2+AP_r)\eta} \\ + a_{14}e^{-a_2\eta} - a_2a_{14}\eta e^{-a_2\eta} \quad (3.25)$$

$$\begin{aligned}
F_2' = & -a_3a_{36}e^{-a_3\eta} - (a_3 + AP_r)a_{24}e^{-(a_3+AP_r)\eta} - (a_2 + AP_r)a_{25}e^{-(a_2+AP_r)\eta} \\
& - (a_2 + a_3)a_{26}e^{-(a_2+a_3)\eta} + a_{27}e^{-a_3\eta} - a_3a_{27}\eta e^{-a_3\eta} - a_2a_{34}\eta e^{-a_2\eta} + a_{29}e^{-a_2\eta} \\
& - a_2a_{29}\eta e^{-a_2\eta} - AP_ra_{35}e^{-AP_r\eta} + a_{32}e^{-AP_r\eta} - AP_ra_{32}\eta e^{-AP_r\eta}
\end{aligned} \tag{3.26}$$

$$\begin{aligned}
\theta_3' = & -AP_ra_{64}e^{-AP_r\eta} - (a_3 + AP_r)a_{51}e^{-(a_3+AP_r)\eta} + a_{52}e^{-(a_3+AP_r)\eta} - (a_3 + AP_r) \\
& a_{52}\eta e^{-(a_3+AP_r)\eta} - (a_2 + AP_r)a_{53}e^{-(a_2+AP_r)\eta} + a_{54}e^{-(a_2+AP_r)\eta} - (a_2 + AP_r)a_{54} \\
& \eta e^{-(a_2+AP_r)\eta} - (a_2 + a_3 + AP_r)a_{55}e^{-(a_2+a_3+AP_r)\eta} - (2a_3 + AP_r)a_{56}e^{-(2a_3+AP_r)\eta} \\
& - (a_3 + 2AP_r)a_{57}e^{-(a_3+2AP_r)\eta} - (2a_2 + AP_r)a_{58}e^{-(2a_2+AP_r)\eta} - (a_2 + 2AP_r)a_{59} \\
& e^{-(a_2+2AP_r)\eta} - 2AP_ra_{60}e^{-2AP_r\eta} + a_{61}e^{-2AP_r\eta} - 2AP_ra_{61}\eta e^{-2AP_r\eta} + a_{62}e^{-AP_r\eta} \\
& - AP_ra_{62}\eta e^{-AP_r\eta} + 2a_{63}\eta e^{-AP_r\eta} - AP_ra_{63}\eta^2 e^{-AP_r\eta}
\end{aligned} \tag{3.27}$$

$$\begin{aligned}
C_3' = & -a_2a_{89}e^{-a_2\eta} - (a_2 + a_3)a_{77}e^{-(a_2+a_3)\eta} + a_{78}e^{-(a_2+a_3)\eta} - (a_2 + a_3)a_{78} \\
& \eta e^{-(a_2+a_3)\eta} - (a_2 + a_3 + AP_r)a_{79}e^{-(a_2+a_3+AP_r)\eta} - (a_2 + 2a_3)a_{80}e^{-(a_2+2a_3)\eta} \\
& - (a_2 + AP_r)a_{81}e^{-(a_2+AP_r)\eta} + a_{82}e^{-(a_2+AP_r)\eta} - (a_2 + AP_r)a_{82}\eta e^{-(a_2+AP_r)\eta} \\
& - (a_2 + 2AP_r)a_{83}e^{-(a_2+2AP_r)\eta} - (2a_2 + a_3)a_{84}e^{-(2a_2+a_3)\eta} - (2a_2 + AP_r) \\
& a_{85}e^{-(2a_2+AP_r)\eta} - 2a_2a_{86}e^{-2a_2\eta} + a_{87}e^{-a_2\eta} - a_2a_{87}\eta e^{-a_2\eta} + 2a_{88}\eta e^{-a_2\eta} \\
& - a_2a_{88}\eta^2 e^{-a_2\eta}
\end{aligned} \tag{3.28}$$

$$\begin{aligned}
F_3' = & -a_3a_{142}e^{-a_3\eta} - (a_3 + AP_r)a_{116}e^{-(a_3+AP_r)\eta} + a_{117}e^{-(a_3+AP_r)\eta} - (a_3 + AP_r) \\
& a_{117}\eta e^{-(a_3+AP_r)\eta} - (a_2 + AP_r)a_{118}e^{-(a_2+AP_r)\eta} + a_{119}e^{-(a_2+AP_r)\eta} - (a_2 + AP_r)a_{119} \\
& \eta e^{-(a_2+AP_r)\eta} - (a_2 + a_3 + AP_r)a_{120}e^{-(a_2+a_3+AP_r)\eta} - (a_2 + a_3)a_{121}e^{-(a_2+a_3)\eta} \\
& + a_{122}e^{-(a_2+a_3)\eta} - (a_2 + a_3)a_{122}\eta e^{-(a_2+a_3)\eta} - 2a_3a_{123}e^{-2a_3\eta} + a_{124}e^{-2a_3\eta} - 2a_3a_{124} \\
& \eta e^{-2a_3\eta} - 2a_2a_{125}e^{-2a_2\eta} - (2a_3 + AP_r)a_{126}e^{-(2a_3+AP_r)\eta} - (a_3 + 2AP_r)a_{127}e^{-(a_3+2AP_r)\eta} \\
& - (2a_2 + AP_r)a_{128}e^{-(2a_2+AP_r)\eta} - (a_2 + 2AP_r)a_{129}e^{-(a_2+2AP_r)\eta} - (a_2 + 2a_3)a_{130}e^{-(a_2+2a_3)\eta} \\
& - 2AP_ra_{131}e^{-2AP_r\eta} + a_{132}e^{-2AP_r\eta} - 2AP_ra_{132}\eta e^{-2AP_r\eta} - (2a_2 + a_3)a_{133}e^{-(2a_2+a_3)\eta} \\
& - AP_ra_{134}e^{-AP_r\eta} + a_{135}e^{-AP_r\eta} - AP_ra_{135}\eta e^{-AP_r\eta} + 2a_{136}\eta e^{-AP_r\eta} - AP_ra_{136}\eta^2 e^{-AP_r\eta} \\
& - a_2a_{137}e^{-a_2\eta} + a_{138}e^{-a_2\eta} - a_2a_{138}\eta e^{-a_2\eta} + 2a_{139}\eta e^{-a_2\eta} - a_2a_{139}\eta^2 e^{-a_2\eta} + a_{140}e^{-a_3\eta} \\
& - a_3a_{140}\eta e^{-a_3\eta} + 2a_{141}\eta e^{-a_3\eta} - a_3a_{141}\eta^2 e^{-a_3\eta}
\end{aligned} \tag{3.29}$$

$$F_1'' = a_3^2a_4e^{-a_3\eta} + A^2P_r^2a_6e^{-AP_r\eta} + a_2^2a_7e^{-a_2\eta} \tag{3.30}$$

$$\begin{aligned}
F_2'' = & a_3^2a_{36}e^{-a_3\eta} + (a_3 + AP_r)^2a_{24}e^{-(a_3+AP_r)\eta} + (a_2 + AP_r)^2a_{25}e^{-(a_2+AP_r)\eta} \\
& + (a_2 + a_3)^2a_{26}e^{-(a_2+a_3)\eta} - 2a_3a_{27}e^{-a_3\eta} + a_3^2a_{27}\eta e^{-a_3\eta} + a_2^2a_{34}e^{-a_2\eta} + a_{29}e^{-a_2\eta} \\
& - 2a_2a_{29}e^{-a_2\eta} + a_2^2a_{29}\eta e^{-a_2\eta} + A^2P_r^2a_{35}e^{-AP_r\eta} - 2AP_ra_{32}e^{-AP_r\eta} + A^2P_r^2a_{32}e^{-AP_r\eta}
\end{aligned} \tag{3.31}$$

$$\begin{aligned}
 F_3'' = & a_3^2 a_{142} e^{-a_3 \eta} + (a_3 + AP_r)^2 a_{116} e^{-(a_3 + AP_r) \eta} - 2(a_3 + AP_r) a_{117} e^{-(a_3 + AP_r) \eta} \\
 & + (a_3 + AP_r)^2 a_{117} \eta e^{-(a_3 + AP_r) \eta} + (a_2 + AP_r)^2 a_{118} e^{-(a_2 + AP_r) \eta} - 2(a_2 + AP_r) \\
 & a_{119} e^{-(a_2 + AP_r) \eta} + (a_2 + AP_r)^2 a_{119} \eta e^{-(a_2 + AP_r) \eta} + (a_2 + a_3 + AP_r)^2 a_{120} e^{-(a_2 + a_3 + AP_r) \eta} \\
 & + (a_2 + a_3)^2 a_{121} e^{-(a_2 + a_3) \eta} - 2(a_2 + a_3) a_{122} \eta e^{-(a_2 + a_3) \eta} + (a_2 + a_3)^2 a_{122} e^{-(a_2 + a_3) \eta} \\
 & + 4a_3^2 a_{123} e^{-2a_3 \eta} - 4a_3 a_{124} e^{-2a_3 \eta} + a_3^2 a_{124} \eta e^{-2a_3 \eta} + 4a_2^2 a_{125} e^{-2a_2 \eta} + (2a_3 + AP_r)^2 \\
 & a_{126} e^{-(2a_3 + AP_r) \eta} + (a_3 + 2AP_r)^2 a_{127} e^{-(a_3 + 2AP_r) \eta} + (2a_2 + AP_r)^2 a_{128} e^{-(2a_2 + AP_r) \eta} \\
 & + (a_2 + 2AP_r)^2 a_{129} e^{-(a_2 + 2AP_r) \eta} + (a_2 + 2a_3)^2 a_{130} e^{-(a_2 + 2a_3) \eta} + 4A^2 P_r^2 a_{131} e^{-2AP_r \eta} \\
 & - 4AP_r a_{132} e^{-2AP_r \eta} + 4A^2 P_r^2 a_{132} \eta e^{-2AP_r \eta} + (2a_2 + a_3)^2 a_{133} e^{-(2a_2 + a_3) \eta} + A^2 P_r^2 a_{134} e^{-AP_r \eta} \\
 & - 2AP_r a_{135} e^{-AP_r \eta} + A^2 P_r^2 a_{135} \eta e^{-AP_r \eta} + 2a_{136} e^{-AP_r \eta} - 4AP_r a_{136} \eta e^{-AP_r \eta} + A^2 P_r^2 a_{136} \eta^2 \\
 & e^{-AP_r \eta} + a_2^2 a_{137} e^{-a_2 \eta} - 2a_2 a_{138} e^{-a_2 \eta} + a_2^2 a_{138} \eta e^{-a_2 \eta} + 2a_{139} e^{-a_2 \eta} - 4a_2 a_{139} \eta^2 e^{-a_2 \eta} + a_2^2 a_{139} \\
 & \eta^2 e^{-a_2 \eta} - 2a_3 a_{140} \eta e^{-a_3 \eta} + a_3^2 a_{140} \eta e^{-a_3 \eta} + 2a_{141} e^{-a_3 \eta} - 4a_3 a_{141} \eta e^{-a_3 \eta} + a_3^2 a_{141} \eta^2 e^{-a_3 \eta}
 \end{aligned} \tag{3.32}$$

#### 4. RESULTS AND DISCUSSIONS

The series for  $\theta$ , its first derivative  $\theta'(0)$  (the wall temperature gradient),  $F'$  (the velocity profile) and  $F''(0)$  (the wall velocity gradient) were evaluated and are presented in Figures 1-7. The general results of the investigations are the imposed magnetic field diminished the velocity field; wall shear, flow rate, and wall heat transfer, also the onset of free convection are retarded while the fluid temperatures and the time required for the flow to each steady state are increased. In addition, sizable influences on the flow and thermal fields can be produced with moderate magnetic field strengths only for liquid metal flows while the effects of induced magnetic fields and Joule heating are very small. The magnetic field strength is to reduce the values of wall shear stress regardless of blowing and suction strength. The magnetic force is known to have a retarding effect; it decreases the wall shear stress. Blowing has a similar effect which used to aid the magnetic field in reducing the wall shear stress. However, suction has an opposite effect and increases the shear stress at the wall opposing the magnetic effect. In case of free convection, suction decreases wall shear stress, this may be because increasing suction will decrease the flow velocity and in turn diminishing the retarding effect of the magnetic field force. In order to get the physical insight into the problem, numerical calculations are carried out for different values of Prandtl number, Hartmann number, Schmidt number and Sherwood number.

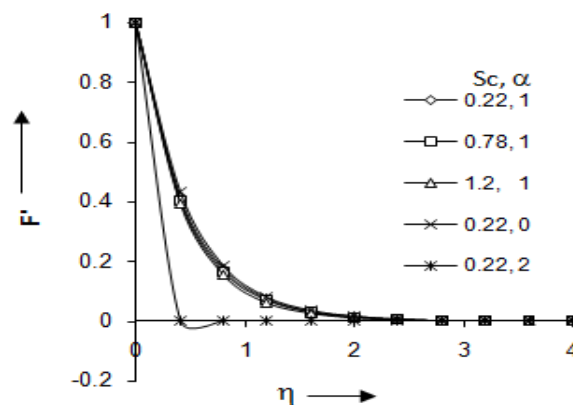
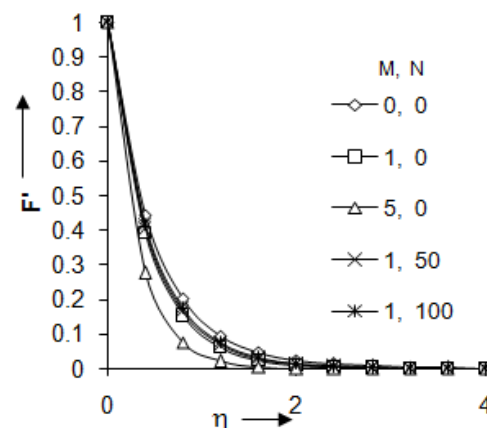


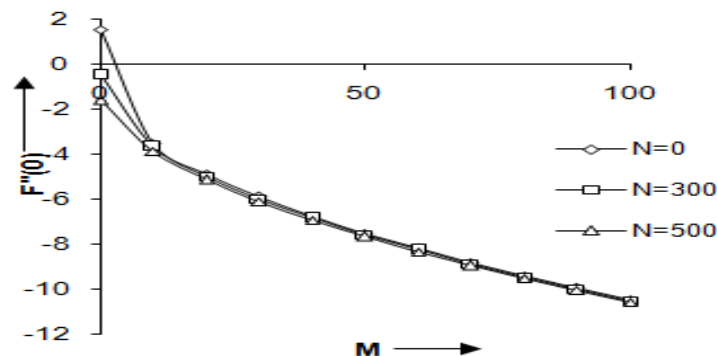
Figure 1: Effects of Sc and  $\alpha$  on Tangential Velocity Profiles, taking  $Pr=0.72$ ,  $Re=50$ ,  $M=1$ ,  $K=5$ ,  $N=20$ ,  $Gr=5$ ,  $A=1$ ,  $F_w=0$ ,  $\varepsilon=1$



**Figure 2: Effects of M and N on Tangential Velocity Profiles, taking  $Pr=0.72$ ,  $Sc=0.2$ ,  $Re=50$ ,  $K=5$ ,  $\alpha=1$ ,  $Gr=5$ ,  $A=1$ ,  $F_w=0$ ,  $\varepsilon=1$**

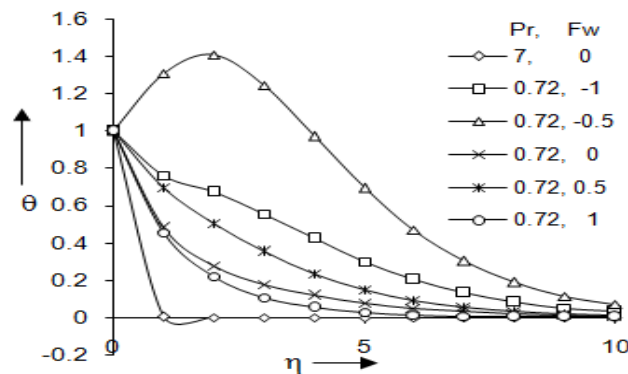
Figure 1 illustrates the influence of Schmidt number  $Sc$  and Porosity parameter  $\alpha$  on the velocity profile in the boundary layer against  $\eta$ . It shows that the velocity profile decreases exponentially as increasing  $\eta$ . It is also observed that the velocity profile decreases as increasing Schmidt number. This causes the concentration buoyancy effects to decrease yielding a reduction in the fluid velocity. The velocity profile also decreases as increasing Porosity parameter. The presence of a porous medium increases the resistance to flow resulting in a decrease in the flow velocity. This behavior is depicted by the decrease in the velocity as  $\alpha$  decreases as shown in figure 1.

Figure 2, illustrates the influence of the Hartmann number  $M$  on the velocity profiles in the boundary layer. Application of magnetic field of an electrically conducting fluid gives rise to a resistive type force called the Lorentz force. This force has the tendency to slow down the motion of the fluid in the boundary layer. Also, the effects on the flow and thermal fields become more so as the strength of the magnetic field increases. This is obvious from the decreases in the velocity profiles presented in Figure 2. It is also seen from Figure 2 that, as expected, the velocity profiles  $f'$  increase monotonically with increasing the buoyancy ratio. The decrease of  $f'$  happens because of an accelerating force, which acts in a direction parallel to the  $\eta$ -axis. As shown, the velocity increases near the plate with increasing buoyancy ratio. This is because the effect of the buoyancy ratio  $N$  is to increase the surface heat and mass transfer rates.



**Figure 3: Effects of N on Non-Dimensional Surface Velocity Gradient, taking  $Pr=0.72$ ,  $Sc=0.2$ ,  $Re=50$ ,  $M=1$ ,  $K=5$ ,  $N=20$ ,  $\alpha=1$ ,  $Gr=5$ ,  $A=1$ ,  $F_w=0$ ,  $\varepsilon=1$**





**Figure 4: Effects of  $Pr$  and  $F_w$  on Temperature Profiles, taking  $Sc=0.2$ ,  $Re=50$ ,  $M=1$ ,  $K=5$ ,  $N=20$ ,  $\alpha=1$ ,  $Gr=5$ ,  $A=1$ ,  $F_w=0$ ,  $\varepsilon=1$**

The effects of buoyancy ratio  $N$  on transport properties are illustrated in Figure 3. The skin friction coefficients reduce with increasing  $N$ . The surface shear stress increases with the magnetic parameter  $M$  due to enhanced Lorentz force which imparts additional momentum into the boundary layer. This reduces the boundary layer thickness which in turn, increases the surface shear stress.

Figure 4 shows the temperature  $\theta(\eta)$  profiles across the boundary layers and different values of the suction/injection parameter  $F_w$  and the Prandtl number  $Pr$ . As mentioned suction corresponding to  $F_w > 0$ , injection to  $F_w < 0$  and  $F_w = 0$  to impermeable plate. It is known that the imposition of wall fluid suction reduces both the hydrodynamic and thermal boundary layers which indicate a reduction in the temperature profiles. However, the exact opposite behavior is produced by the imposition of wall fluid blowing or injection. These behaviors are clear from Figure 4. It is also observed that the magnitude of temperature for air ( $Pr=0.72$ ) is greater than that of water ( $Pr=7.0$ ). This is due to fact that the thermal conductivity of fluid decreases with increasing  $Pr$ , result a decrease in thermal boundary layer thickness.

Figure 5 presents the non-dimensional wall temperature gradient  $\theta'(0)$  □ local Nusselt number  $-\theta'(M, 0)$  at selected values of  $N$ . Increasing the buoyancy ratio will cause the enhancement in the heat transfer at small values of  $M$ . Increasing  $N$  will cause the non-dimensional wall temperature gradient  $\theta'(0)$ . The local Nusselt number is found to be decreased more rapidly at a large value of  $N$ . Figure 5 shows clearly that the presence of the magnetic field gives a reduction of the local Nusselt number, in terms of  $\theta'(M, 0)$  In a manner that the local Nusselt number is to be decreased as  $M$  increases. Figure 5 illustrates the effect of mass transfer  $F_w$  on the dimensionless temperature gradient profiles. It should be noted here that positive values of  $F_w$  indicate fluid suction at the surface while negative values of  $F_w$  correspond to fluid blowing or injection at the wall. The effect of suction is to make the velocity and temperature distribution more uniform within the boundary layer. Imposition of fluid suction at the surface has a tendency to reduce both the hydrodynamic and thermal thickness of the boundary layer where viscous effects dominate. This result in increasing the non-dimensional surface temperature gradient is shown in Figure 5. On the other hand, the opposite result is obtained from fluid blowing  $F_w < 0$  at the wall, a decrease in the non-dimensional surface temperature gradient.

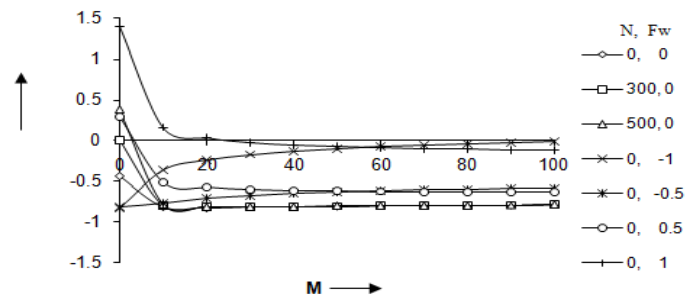


Figure 5: Effects of  $N$  and  $F_w$  on Non-Dimensional Wall Temp. Gradient, Taking  $Sc=0.2$ ,  $Re=50$ ,  $M=1$ ,  $K=5$ ,  $\alpha=1$ ,  $Gr=5$ ,  $A=1$ ,  $\varepsilon=1$ ,  $Pr=0.72$

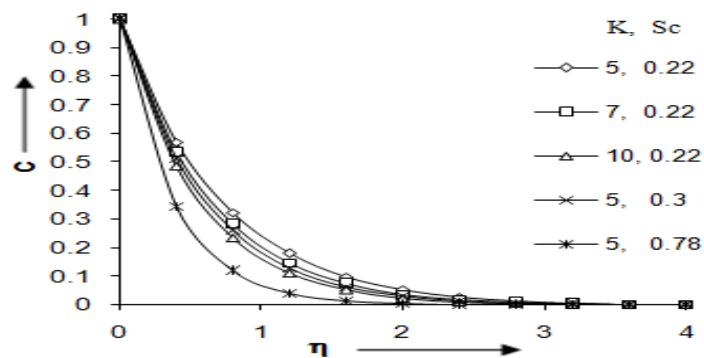


Figure 6: Effects of  $K$  and  $Sc$  on Concentration Profiles, Taking  $Pr=0.72$ ,  $Re=50$ ,  $M=1$ ,  $N=20$ ,  $\alpha=1$ ,  $Gr=5$ ,  $A=1$ ,  $F_w=0$ ,  $\varepsilon=1$

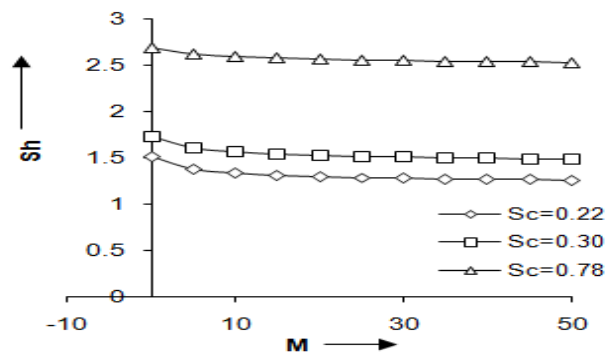


Figure 7: Effects of  $Sc$  on Sherwood Number, Taking  $Pr=0.72$ ,  $Re=50$ ,  $K=5$ ,  $N=20$ ,  $\alpha=1$ ,  $Gr=5$ ,  $A=1$ ,  $F_w=0$ ,  $\varepsilon=1$

Figure 6 illustrates the influence of Schmidt number  $Sc$  on the concentration. As Schmidt number  $Sc$  increases, the mass transfer rate increases. Hence, the concentration decreases with increasing  $Sc$ . It is evident from this figure that the concentration  $C$  takes its limiting value  $C_\infty$ , for higher values of the dimensionless distance  $\eta$ . From this figure, we observe that when the concentration difference  $\delta C$  is maintained constant, the dimensionless concentration profile decreases, in the sense that the values of the Schmidt number increases. It is also concluded that concentration profile decreases as increasing chemical reaction parameter  $K$ .

The effect of Schmidt number on the Sherwood number is depicted in Figure 7. It is clearly seen that the influence of  $Sc$  of the local Sherwood number is considerable. The results of figure indicate that, a larger  $SH$  is experienced for a system with a larger  $Sc$ . That is, the mass transfer rate increases with the increase in Schmidt number. This is due to the fact that a larger Schmidt number corresponds to a small binary diffusion coefficient for a given mixture and to a thinner concentration boundary layer thickness relative to the flow boundary layer thickness. This results in a larger mass transfer rate at the duct wall or a larger Sherwood number.

## 5. NOMENCLATURE

$T_0$  - The temperature of the plate,  $K$ ;  $T$  - the temperature in the boundary,  $K$

$T_w$  - The temperature at wall,  $K$ ;  $T_\infty$  - Free stream temperature,  $K$

$u, v$  - Velocity components in X and Y direction respectively,  $m.s^{-1}$

$C'$  - Concentration in the fluid,  $mol.m^{-3}$ ;  $C'_w$  - Concentration at the wall,  $mol.m^{-3}$

$C'_\infty$  - Free streaming concentration,  $mol.m^{-3}$ ;  $C$  - Dimensionless concentration

$t'$  - The time,  $s$ ;  $B, a, b$  - constants;  $g$  - the acceleration due to the gravity,  $m.s^{-1}$

$C_p$  - The heat capacity of the fluid,  $J.Kg^{-1}.K^{-1}$ ;  $B_0$  - the magnetic induction

$a_0 = \frac{\kappa}{\rho C_p}$  (Thermal Diffusivity);  $Pr$  - the Prandtl number;

$K_1$  - The chemical reaction parameter;  $K$  - Non-dimensional chemical reaction parameter

$M$  - The magnetic parameter;  $Re$  - the Reynold number;  $N$  - the buoyancy ratio

$Gr_r$  - The thermal Grashof number;  $Sh$  - the Sherwood number;  $Sc$  - the Schimdt number

$D$  - Mass diffusion coefficient,  $m^2.s^{-1}$ ;  $F$  - the velocity

## Greek Letters

$\square'$  - The porosity parameter;  $\square$  - non-dimensional porosity parameter

$\beta$  - The volumetric coefficient of thermal expansion,  $K^{-1}$

$\beta_c$  - Volumetric coefficient of expansion with concentration,  $K^{-1}$

$\rho$  - The density of the fluid,  $Kg.m^{-3}$ ;  $\theta$  - Dimensionless temperature

$\mu$  - The coefficient of viscosity, Pa.s;  $\nu$  - the kinematics viscosity,  $m^2.s^{-1}$

$\sigma$  - The electrical conductivity;  $K$  - the coefficient of thermal conductivity,  $Wm^{-1}K^{-1}$

## 6. CONCLUSIONS

In this paper, the effect of heat and mass transfer in a hydro-magnetic flow of a moving permeable vertical surface was analyzed. In the formulation of the problem, the system of momentum, heat and mass conservation equations were reduced to some parameter problem by introducing suitable transformation variable. The resulting transformed governing equations were then solved using a perturbation technique. Results on the different profiles were presented for various governing parameters. We observed that the presence of a porous medium increases the resistance to flow resulting in a decrease in the flow velocity and the velocity profiles  $F'$  increase monotonically with increasing the buoyancy ratio due to increase the surface heat and mass transfer rates and decrease in the increase of the Hartmann number  $M$ .

## REFERENCES

1. Aziz, A. and Na, T. Y. (1984). *Perturbation methods in heat transfer*. Berlin: Springer-Verlag;. pp. 1–184.
2. Kennet Cramer, R. and Shih-I Pai. (1973). *Magneto fluid dynamics for engineers and applied physicists*. Washington, D. C.: Scripta Publishing Company, McGraw-Hill Book Company; pp-166–167.
3. Tsou, F. K., Sparrow, E. M. and Goldstein, R. J. (1967). Flow and heat transfer in the boundary layer on a continuous moving surface. *Int J Heat Mass Transfer* Vol.10, pp-219–235.
4. Chen, T. S. and Strobel, F. A., (1980). Buoyancy effects in boundary layer adjacent to a continuous, moving horizontal flat plate. *Trans ASME J Heat Transfer* Vol.102, pp-170–172.
5. Chakrabarti, A. and Gupta, A. S., (1979). Hydromagnetic flow and heat transfer. Over a stretching sheet. *Quart Appl Math.* Vol.37, pp-73–78.
6. Vajravelu, K. and Hadjinicolaou, A., (1997). Convective heat transfer in an electrically conducting fluid at a stretching surface with uniform free stream. *Int J Eng Sci* Vol.35, pp-1237–1244.
7. Cheng, W. T. and Huang, C. N., (2004). Unsteady flow and heat transfer on an accelerating surface with blowing or suction in the absence and presence of a heat source or sink. *Chem Eng Sci.* Vol. 59, pp-771–780.
8. Xu, H. and Liao, S. J., (2005). Analytic solutions of magnetohydrodynamic flows of non-Newtonian fluids caused by an impulsively stretching plate. *J Non-Newton Fluid Mech.* Vol.159, pp-46–55.
9. Abdelkhalek, M M., (2007). Thermal radiation effects on hydromagnetic flow. *CAMES.* Vol. 14(3), pp-471–484.
10. Abdelkhalek, M M., (2006). Unsteady MHD convection and mass transfer flow of micropolar fluids past a vertical permeable moving plate with heat absorption. *Indian J Phys.* Vol. 80(6), pp-625–635.
11. Abdelkhalek, MM., (2008). Mixed convection in a square cavity by a perturbation technique. *Comput Mater Sci.*, Vol.42, pp-212–219.
12. Wilks, G. and Hunt, R., (1984). Magneto-hydrodynamic free convection flow about a semi-infinite plate at whose surface the heat flux is uniform. *J Appl Math Phys.* Vol.35, pp-34–49.
13. Watanabe, T. and Pop, I., (1993). Magneto-hydrodynamic free convection flow over a wedge in the presence of a transverse magnetic field. *Int Commun Heat Mass Transfer.* Vol.20, pp-871–81.
14. D. Babu Reddy & G. S. S. Raju (2017). “Hall Current Effects on MHD Free Convective Heat and Mass Transfer Flow Past an Oscillating Vertical Porous Plate in the Presence of Radiation, Thermal & Mass Diffusion with Chemical Reaction”. *IJMCAR*

15. Kafoussias, NG. (1992). MHD free convective flow through a non homogeneous porous medium over an isothermal cone surface. *Mech Res Commun*. Vol.19, pp-89–99.
16. Bakier, A. Y., Mansour, M. A., Gorla, R. S. R. and Ebiana, A. B., (1997). Non-similar solutions for free convection from a vertical plate in porous media. *Heat Mass Transfer*. Vol.33, pp-145–148.
17. N. Senapati, R. K. Dhal & K. Ray (2013). “Effect of Chemical Reaction on MHD Free Convection on Kuvshinshki Fluid through Porous Medium in Presence of Heat Radiation with Constant Heat and Mass Flux Across Moving Plate”. *International Journal of Applied Mathematics & Statistical Sciences*. Vol(2). pp 45-52.
18. Pop, I. and Postelnicu, A., (1999). Similarity solutions of free convection boundary layers over vertical and horizontal surface porous media with internal heat generation. *Int Commun Heat Mass Transfer*. Vol.26, pp-1183–91.
19. Grubka, L. J. and Bobba, K. M., (1985). Heat transfer characteristics of a continuous stretching surface with variable temperature ASME. *J Heat Transfer*. Vol.107, pp-248–250.
20. Ali, M. E., (1994). Heat transfer characteristics of a continuous stretching surface. *Warme Stoffübertragung*. Vol.29, pp-227–234.
21. Rajendra Kumar Dhal & Sanjay Kumar Jena (2016). « Effect of Chemical Reaction on MHD Free Convection Flow Past an Exponentially Accelerate Porous Plate with Variable Temperature Embedded in Porous Medium” Vol(4). pp 131-144.
22. Takhar, H. S., Raptis, A. A. and Perdikis, C. P., (1986). MHD asymmetric flow past a semi-infinite moving plate. *Acta Mech*. Vol. 65, pp-287–290.
23. Yih, K. A., (1999). Free convection effect on MHD coupled heat and mass transfer of a moving permeable vertical surface, *Int Commun Heat Mass Transfer*. Vol. 26, pp-95–104.
24. Sudheer Babu, M., Satya Narayana, P. V., Sankar Reddy, T. and Umamaheswara Reddy D. (2011). Radiation and chemical reaction effects on an unsteady MHD convection flow past a vertical moving porous plate embedded in a porous medium with viscous dissipation, *Advances in Applied Science Research*, Vol. 2 (5), pp-226-239.
25. Reddy, S. T., Reddy, S. P. O., Raju, M. C. and Varma, S. V. K., (2012). MHD free convection heat and mass transfer flow through a porous medium bounded by a vertical surface in presence of hall current, *Advances in Applied Science Research*, Vol.3(6), pp-3482-3490.

